



Cite this: *Nanoscale Horiz.*, 2023,
8, 1333

Received 31st May 2023,
Accepted 26th July 2023

DOI: 10.1039/d3nh00213f

rsc.li/nanoscale-horizons

MXene-based nanomaterials with enzyme-like properties for biomedical applications

Rong Yang,^{id}*^{ab} Shiqi Wen,^{ab} Shuangfei Cai,^{id}*^a Wei Zhang,^{*c} Ting Wu^a and Youlin Xiong^a

Recently, great progress has been made in nanozyme research due to the rapid development of nanomaterials and nanotechnology. MXene-based nanomaterials have gained considerable attention owing to their unique physicochemical properties. They have been found to have high enzyme-like properties, such as peroxidase, oxidase, catalase, and superoxide dismutase. In this mini-review, we present an overview of the recent progress in MXene-based nanozymes, with emphasis on their synthetic methods, hybridization, bio-catalytic properties, and biomedical applications. The future challenges and prospects of MXene-based nanozymes are also proposed.

1. Introduction

Since the discovery of the peroxidase-like activity of Fe₃O₄ nanoparticles (NPs) in immunoassays, great advances have

been made in nanozyme research.^{1–4} Nanozymes are functional nanomaterials with enzyme-like properties. Compared to natural enzymes, nanozymes exhibit several advantages, such as inexpensive preparation, high stability under different environmental conditions (low pH, high temperature or the presence of salt), easy surface functionalization, better reusability, and robust catalytic activities. Researchers have found that various nanomaterials have enzyme-like activities, such as metal NPs, metal oxides, metal chalcogenides and carbon-based nanomaterials.^{5–11} Two-dimensional (2D) nanomaterials are a very important class of materials.¹² Since the discovery of graphene in 2004,¹³ a lot of 2D nanomaterials, including transition metal dichalcogenides (TMDs),¹⁴ ultrathin metal

^a CAS Key Laboratory for Biomedical Effects of Nanomaterials and Nanosafety, Center of Materials Science and Optoelectronics Engineering, CAS Center for Excellence in Nanoscience, National Center for Nanoscience and Technology, University of Chinese Academy of Sciences, Beijing 100190, China.
E-mail: yangr@nanoctr.cn, caisf@nanoctr.cn

^b Sino-Danish College, Sino-Danish Center for Education and Research, University of Chinese Academy of Sciences, Beijing 100049, China

^c Institute of Applied Physics and Computational Mathematics, Beijing 100088, China. E-mail: zhang_wei@iapcm.ac.cn



Rong Yang

Dr Rong Yang is a Professor at the National Center for Nanoscience and Technology of China (NCNST). Dr Yang received her PhD from Ohio University, USA, in 2006. After that, she worked as a postdoctoral researcher in the Department of Chemical Engineering and Materials Science at the University of Minnesota from 2006 to 2007. She joined NCNST in 2008. She is currently conducting interdisciplinary research, linking materials, chemistry, biology and physics. She

is also working on the design and development of multi-functional nanomaterials for human and environmental health applications. She has published more than 90 papers in international high-level academic journals.



Shiqi Wen

Shiqi Wen is a Master's degree student jointly trained at the National Center for Nanoscience and Technology, and the Sino-Danish College of the University of the Chinese Academy of Sciences (UCAS). She received her BS degree in Chemistry from Beijing Jiaotong University in 2019. In the same year, she joined Professor Rong Yang's group at the National Center for Nanoscience and Technology of China. Her research focuses on

the controllable synthesis of MXene-based nanocomposites for antibacterial applications.

nanomaterials,¹⁵ graphitic carbon nitride ($g\text{-C}_3\text{N}_4$),¹⁶ and metal–organic frameworks (MOFs),¹⁷ have attracted considerable attention in many research fields. With their single-atom layers or several-atom-thick layers, 2D nanomaterials have very high surface areas, together with their unique physicochemical properties and therefore, have brought about enormous research interest in biomedical fields, including biosensing, bioimaging, cancer therapy, and antibacterial agents.^{18–21}

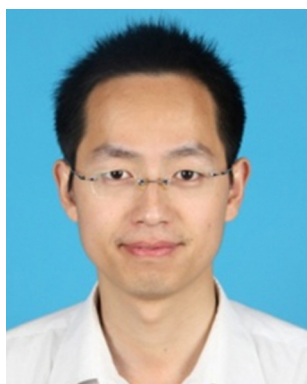
Researchers have found that carboxyl-modified graphene oxide (GO) nanosheets (NSs) can mimic horseradish peroxidase (HRP), which were further developed as a glucose biosensor based on the peroxidase (POD)-like activity.²² Subsequently, lots of 2D nanomaterials with enzymatic activities have been reported.^{23–28}

Very recently, transition metal carbides/nitrides/carbonytrides (MXenes), as a relatively new family of 2D compounds, have attracted enormous interest.^{29–36} They have a general chemical formula of $\text{M}_{n+1}\text{X}_n\text{T}_x$, where M is an early transition metal element (e.g., Ti, Zr, V, Nb, and Mo); $n = 1–3$; X represents C and N; and T_x stands for surface terminations (e.g., $-\text{OH}$, $-\text{O}$, $-\text{F}$, and $-\text{Cl}$). MXenes have high conductivity, tunable surface

terminations, and controllable thickness and thus have been employed in various fields, such as energy storage, catalysis, and drug delivery. For example, as one type of MXene, Ti_3C_2 NSs exhibit several distinguished characteristics as follows: (1) they are terminated by hydrophilic functionalities, such as $-\text{OH}$ and $-\text{O}$ on their surfaces; thus, they have good water dispersibility and can be further functionalized with different chemical groups. (2) The metallic conductivity and the exposed terminal Ti with multiple valence states provide them with charge-carrier transfer and redox reactivity properties. (3) They are environmentally friendly. (4) Ti_3C_2 NSs possess intrinsic POD-like activity.³⁷

Although several reviews have been presented on the synthesis, properties, and applications of MXene-based nanocomposites,^{29,32,35,36} relevant reviews on the advances in the enzyme-like activities of MXene-based nanomaterials are limited.

In this mini-review, we summarize the recent progress in MXenes with enzyme-like properties for biomedical applications. First, we briefly introduce the synthesis and functionalization strategies of MXenes. Then, we discuss the enzyme-like properties of MXenes. After that, we summarize the recent progress of MXene-based nanozymes in various biomedical applications,



Shuangfei Cai

Dr Shuangfei Cai is an Associate Professor at the National Center for Nanoscience and Technology of China. Dr Cai received his PhD from the Beijing Institute of Technology in 2011. After that, he worked as a postdoctoral researcher in the Department of Chemistry at Tsinghua University from 2011 to 2013. He joined the NCNST in 2013. He is currently working on the preparation, catalytical properties and biosensing applications of nanomaterials. He has published

more than 40 papers in international high-level academic journals.



Wei Zhang

Dr Wei Zhang is a Professor at the Institute of Applied Physics and Computational Mathematics in China. Dr Zhang received his PhD from the Institute of Theoretical Physics, Chinese Academy of Sciences in 1998. His research interest is focused on condensed matter physics and nanomaterials. He has published more than 100 papers in international high-level academic journals.



Ting Wu

Ting Wu is currently a PhD candidate with a major in nanoscience and technology at the National Center for Nanoscience and Technology under the supervision of Prof. Rong Yang. She obtained her Bachelor's degree in chemistry from the Shandong Agricultural University in 2019. Her research focuses on the preparation of functional nanomaterials for biomedical applications.



Youlin Xiong

Youlin Xiong is currently a PhD candidate with a major in nanoscience and technology at the National Center for Nanoscience and Technology under the supervision of Prof. Rong Yang. He obtained his Bachelor's degree at the School of Materials Science and Engineering from the Jiangsu University. His research focuses on the controllable synthesis of MXene-based nanocomposites for human and environmental health applications.

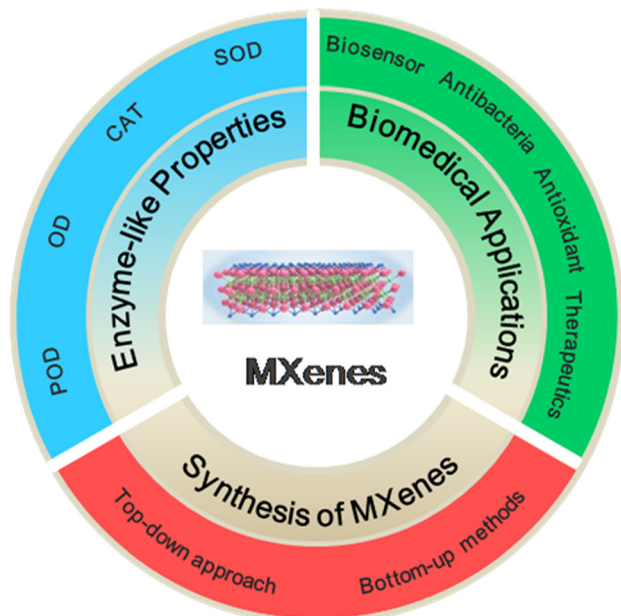


Fig. 1 MXene-based nanomaterials with enzyme-like activities for biomedical applications.

ranging from biosensors, therapeutics and antibacterial agents to antioxidants (Fig. 1). Finally, we address the prospects and challenges of MXene-based nanozymes.

2. Synthesis and surface modification of MXene nanomaterials

2.1. Synthetic approaches to MXenes

The bottom-up and top-down methodologies are commonly used for the synthesis of 2D nanomaterials including MXenes.^{38,39} The former includes classical chemical vapor deposition (CVD) and wet-chemical synthesis. CVD has been widely used to prepare conventional 2D materials. Ultrathin Mo₂C films were the first MXenes synthesized by the CVD method.⁴⁰ Xu *et al.* used methane as the carbon source and copper/molybdenum foil as the substrate to synthesize 2D tungsten carbide (WC), molybdenum carbide (MoC₂) and tantalum carbide (TaC) films⁴⁰ by CVD at about 1085 °C. The as-synthesized thin films had high crystallinity but the materials prepared by this method lack surface functional groups and need further surface modification.

The top-down route is based on exfoliation processes. Since the exfoliation of Ti₃C₂T_x from the corresponding MAX phase (Ti₃AlC₂) materials (as shown in Fig. 2),²⁹ various methods have been developed to obtain 2D MXenes with ultrathin layers.^{29–37,41–43}

The delamination of MXenes can hardly be achieved by mechanical exfoliation due to the metallic bindings between M and A.⁴⁴ Thus, the efficient and selective etching of the MAX phase and intercalation/sonication is required. Some of the most representative synthesis approaches are listed below:

2.1.1. Fluorine-based etching

Hydrofluoric acid (HF) etching. The selective etching of MAX phase materials using HF is the most commonly used

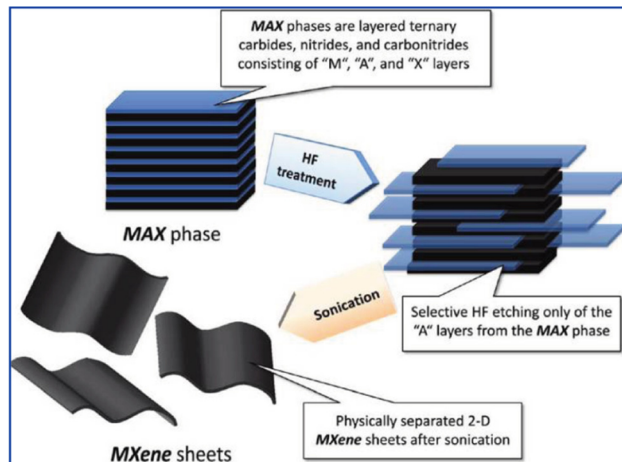
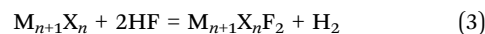
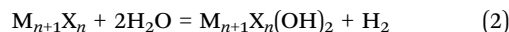
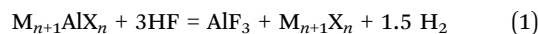


Fig. 2 Schematic showing the exfoliation process of MAX phases and the formation of MXenes. Adapted with permission from ref. 29. Copyright (2012) The American Chemical Society.

method.^{32,45} Here, MAX phase powders are immersed in the HF solution with stirring for a period. During this process, the M-A bonds are broken and the final products contain –F, –OH, and –O-rich surfaces with the introduction of HF. The reactions during HF etching on Al-containing MAX phase precursors were proposed by Gogotsi and Barsoum *et al.*:⁴⁶



The value of n of each MAX phase precursor determines the etching time and HF concentration in exfoliation.

After HF treatments, the multilayer MXenes with accordion-like structures were obtained. Ultrasonication was required to further delaminate and prepare few-layer or single-layer MXenes. MXene NSs obtained through this method often have lamellar structures with defect-rich surfaces. Besides Ti₃C₂, other MXenes including V₄C₃, V₂C, Nb₄C₃, Hf₃C₂ and Ti₂N,^{47–51} were also successfully obtained using the HF etching method.

In situ HF etching. To avoid the direct use of corrosive HF, another route was developed by generating *in situ* HF during the etching process. Ghidui *et al.*⁵² obtained single-layered Ti₃C₂T_x nanosheets by adding hydrochloric acid (HCl) and fluoride salts (*i.e.*, lithium fluoride, LiF) followed by sonication. In addition to LiF, potassium fluoride (KF), sodium fluoride (NaF), and ammonium fluoride (NH₄F)^{52–54} are also potential fluoride salts that can be used. Compared to HF etching, the cooperation of HCl and fluoride salts provides a milder exfoliation effect and the MXenes obtained have larger lateral dimensions, fewer surface defects and good electrical performance.

Ammonium hydrogen bifluoride (NH₄HF₂) etching. The Barsoum group⁵⁵ etched Al layers in Ti₃AlC₂ using NH₄HF₂ instead of HF *via* a mild exfoliation route. The advantage of this approach is that the etching of Al and the intercalation of NH₄⁺ cations and NH₃ into

the delaminated sheets could happen simultaneously, thus simplifying the procedures.

2.1.2. Fluorine-free etching. Since the properties of MXenes are strongly dependent on their surface groups and fluorine-based etching induces primarily F-rich surfaces,⁵⁶ great efforts have been made to achieve fluorine-free synthesis.

Lewis acidic molten salt etching. In 2019, the Huang group⁵⁷ substituted the Al-layer in the MAX phase with an atomic Zn layer, and then extracted the Zn layer using zinc chloride (ZnCl_2) salts, obtaining Cl-terminated MXenes. Molten ZnCl_2 showed strong Lewis acidity, in which Zn^{2+} resembled the H^+ in HF, and Cl^- coordinated with M atoms.⁵⁷ They further generalized the route for other MAX phase materials with the A layer of Al, Si and Ga, as well as multiple Lewis acidic molten salts (*e.g.*, ZnCl_2 , FeCl_2 , CuCl_2 and AgCl , *etc.*),⁵⁸ providing a general fluorine-free route for the preparation of MXenes.

Alkali-assisted etching. Researchers have employed alkali as the etchant for efficient Al-layer removal. Li *et al.*⁵⁹ immersed Ti_3AlC_2 powder in sodium hydroxide (NaOH) solution under hydrothermal conditions and synthesized multilayer F-free MXenes. Another applicable route utilizes organic alkali. For example, the introduced tetramethylammonium hydroxide (TMAOH) can induce the formation of aluminum oxo-anion, $\text{Al}(\text{OH})_4^-$, and modified $\text{Ti}_3\text{C}_2\text{T}_x$ layers.⁶⁰ In this process, the bulk cation TMA^+ facilitates the intercalation and thus results in an increased interlayer spacing of the MXene NSs.

2.2. Surface modification of MXene-based nanomaterials

Single- or few-layer MXenes are not very stable in water or environments with oxygen.^{29–31} Also, the oxidation of MXene solutions may be accelerated when exposed to light. Surface modification of MXenes with functionalized species is a useful strategy to increase their stability, integrate their functionalities and promote synergistic effects.

MXenes have high surface area and hydrophilic properties. They can be modified with various materials such as polymers,^{61–63} carbon-based materials,⁶⁴ metal sulfides/oxides^{65,66} and metals.^{67–69} For example, Geng's group obtained titanium carbide (Ti_3C_2) nanosheets terminated with $\text{Al}(\text{OH})_4^-$ by intercalation of Ti_3AlC_2 with tetramethylammonium (TMAOH) and then modified them with polyethylene glycol (PEG) molecules. The functionalized Ti_3C_2 NSs were found to have excellent stability in physiological solutions.⁶¹ Shi's group reported the modification of Ti_3C_2 NSs with soybean phospholipid by adsorption to improve their dispersibility and stability in physiological solution for biomedical applications. The functionalized Ti_3C_2 NSs demonstrated enhanced permeability, stable circulation, and retention ability.⁶²

Chen *et al.* found that the co-doping of nitrogen and sulfur could promote the peroxidase-like and electrochemical activity of Ti_3C_2 NSs.⁶⁷ The rare earth elements could also be incorporated into the MXenes.^{68,69} 2D rare-earth metal carbides (MXenes) are attractive due to their novel electronic and magnetic properties and their potential as scalable 2D magnets. Iqbal *et al.*⁶⁸ have reported experimental and theoretical results

on the structural, optical and magnetic properties of un-doped and La-doped $\text{Ti}_3\text{C}_2\text{T}_x$ MXene obtained by coprecipitation. Their results indicated the coexistence of ferromagnetic- anti-ferromagnetic phases. In another study, Yao *et al.*⁶⁹ used density functional theory with the Hubbard U correction to characterize the structure, termination, and magnetism in an out-of-plane ordered rare-earth containing $\text{M}_3\text{C}_2\text{T}_x$ MXene, $\text{Mo}_2\text{NdC}_2\text{T}_2$ ($\text{T} = \text{O}$ or OH). They found that both $\text{Mo}_2\text{NdC}_2\text{O}_2$ and $\text{Mo}_2\text{NdC}_2(\text{OH})_2$ were magnetic. These results showed an increase in magnetism due to the rare-earth element doping of MXene.

Various metal nanoparticle/MXenes hybrids have also been reported, including $\text{Au}/\text{Ti}_3\text{C}_2$,^{34,70–72} $\text{Pt}/\text{Ti}_3\text{C}_2$,⁷³ and $\text{Au}-\text{TiO}_2@ \text{Ti}_2\text{C}$.⁷⁴ The *in situ* growth route was adopted by several groups for the synthesis of Au and Pt NPs on Ti_3C_2 NSs,^{34,70–73} *via* physical and chemical processes. For example, Tang *et al.*⁷¹ fabricated $\text{Ti}_3\text{C}_2@ \text{Au}$ -PEG nanocomposites through a seed-mediated growth method together with the surface modification of sulfhydryl polyethylene glycol (SH-PEG). By electrostatic adsorption, Wang *et al.*⁷² fabricated $\text{Ti}_3\text{C}_2\text{T}_x$ -supported Au NPs, which were prepared by liquid-phase reduction of the Au precursors in the presence of sodium citrate and sodium borohydride. Using isopropanol as the reducing agent, Wojciechowski *et al.*⁷⁴ synthesized the $\text{Au}-\text{TiO}_2@ \text{Ti}_2\text{C}$ under stirring for two days, in which $\text{Ti}(\text{O}_i-\text{P}_i)_4$ and Au^{3+} ions acted as precursors. However, these methods usually involve a multi-step procedure, a long time and the use of surface stabilizers/reductants.

In a recent study, our group reported a facile strategy for constructing the $\text{Au}@ \text{Ti}_3\text{C}_2\text{T}_x$ heterostructure³⁴ as shown in Fig. 3. The $\text{Ti}_3\text{C}_2\text{T}_x$ NSs were delaminated through etching and sonication and acted as a reductant for the *in situ* reduction of $\text{HAuCl}_4 \cdot x\text{H}_2\text{O}$, producing “naked” Au NPs without any stabilizers. During the synthesis, $\text{HAuCl}_4 \cdot x\text{H}_2\text{O}$ was reduced to metallic Au by the redox reaction promoted by the negatively charged surface terminations, the low valence Ti species and surface defects in the $\text{Ti}_3\text{C}_2\text{T}_x$ supports. The generated Au

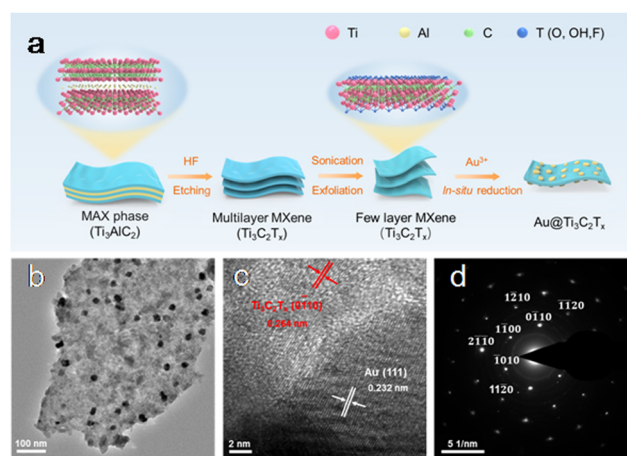


Fig. 3 (a) Illustration of the construction of the $\text{Au}@ \text{Ti}_3\text{C}_2\text{T}_x$; (b) TEM image; (c) HRTEM image; (d) SAED pattern. Adapted with permission from ref. 34. Copyright (2022) Royal Society of Chemistry.

clusters as seeds adhered to the $\text{Ti}_3\text{C}_2\text{T}_x$. As the reaction proceeded, the Au seeds evolved into large-sized NPs.³⁴

3. Enzymatic properties of MXene-based nanozymes

3.1. Peroxidase and oxidase-like properties of MXene-based nanozymes

Peroxidases and oxidases (ODs) are oxidative enzymes in biosystems, which activate $\text{H}_2\text{O}_2/\text{O}_2$ to catalyze the oxidation of the respective substrates under mild conditions. There are many reported studies on the POD/OD-like properties of MXene-based nanomaterials.^{37,75–84} Similar to horseradish peroxidase (HRP), the MXene-based nanomaterials³⁷ could also catalyze the reaction of the peroxidase substrate 3,3',5,5'-tetramethylbenzidine (TMB) in the presence of H_2O_2 to produce a blue-colored reaction. The catalytic activity was dependent on temperature, pH, and H_2O_2 concentration (Fig. 4).

Besides the intrinsic catalytic activity, MXenes can be used as good supports for catalytic processes due to their large specific areas. Also, they have rich physicochemical properties and have the potential to further promote the POD catalysis and stability of the supported nanoparticles. For example, Geng *et al.*⁷³ constructed $\text{Ti}_3\text{C}_2/\text{Pt}$ nanomaterials with synergistically enhanced POD-like activity. The optimal POD-like activity of $\text{Ti}_3\text{C}_2/\text{Pt}$ was 6 times higher than Pt in the dark, and 7.9 times higher than Pt under illumination. This catalytic enhancement was attributed to the combination of the strong interfacial electron effect and unique photothermal effect of Ti_3C_2 .

Recently, Li *et al.*⁷⁵ reported the synthesis of MXene- $\text{Ti}_3\text{C}_2/\text{CuS}$ nanocomposites with POD-like activity using a simple hydrothermal approach. Compared with the individual Ti_3C_2 nanosheets or CuS nanoparticles, the $\text{Ti}_3\text{C}_2/\text{CuS}$ showed a synergistically enhanced POD-like activity and could be used as an efficient peroxidase-mimic to catalyze the TMB oxidation in the presence of H_2O_2 , causing a blue color change.

In another study, Li *et al.*⁷⁶ found that the Ti_3C_2 sheets had intrinsic POD-like activity, which could be enhanced by single-stranded DNA (ssDNA) adsorption. Hence, a simple label-free sensing strategy was developed for the colorimetric detection of biomolecules.

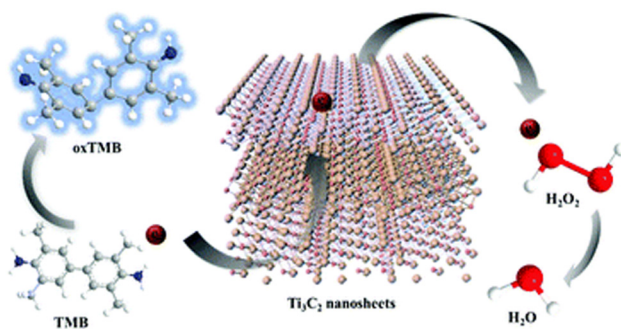


Fig. 4 The peroxidase-like activity of Ti_3C_2 nanosheets. Adapted with permission from ref. 37. Copyright (2020) Royal Society of Chemistry.

Oxidases catalyze oxidation with O_2 as the oxygen source. Jin *et al.*⁷⁷ prepared quantum dots of TiO_2 loaded on carbon ($\text{TiO}_2/\text{C-QDs}$) as an active oxidase-mimicking nanozyme by the hydrothermal treatment of the tiny and few-layered $\text{Ti}_3\text{C}_2\text{T}_x$ MXene nanosheets. Based on this, a fast and sensitive colorimetric method was established for the specific detection of GSH.

3.2. Superoxide dismutase (SOD)- and catalase (CAT)-like properties

SODs and CATs are antioxidant enzymes. They are important in maintaining redox balance in living organisms by scavenging excess ROS. Feng *et al.*⁸⁵ constructed 2D vanadium carbide (V_2C) nanozymes. These nanozymes effectively catalyze the transformation of $\text{O}_2^{\bullet-}$ into H_2O_2 and O_2 , which are produced by decomposition into O_2 and H_2O and the scavenging of $\cdot\text{OH}$, thereby inhibiting the elevation of the intracellular ROS levels. Following a similar mechanism described above, several MXene-based nanomaterials displayed SOD and CAT-like activities.^{86–91} Ren *et al.*⁹¹ prepared the polyvinylpyrrolidone (PVP)-modified Nb_2C nanosheets by liquid-phase exfoliation. They discovered that the obtained Nb_2C had SOD-like properties. The SOD-like activity of Nb_2C nanosheets originated from the surface oxidation process.

3.3. Multiple enzymatic activities of MXene-based nanozymes

Several MXene-based nanozymes were found to have multiple enzymatic activities. For example, the V_2C -based nanozymes⁸⁵ had six kinds of enzyme-like properties, including SOD, CAT, POD, glutathione peroxidase (GPx), thiol peroxidase (TPx) and haloperoxidase (HPO). Based on these properties, the as-constructed V_2C -based nanozymes not only possessed high biocompatibility but also exhibited robust *in vitro* cytoprotection against oxidative stress (Fig. 5).

3.4. Regulating the enzymatic activities of MXene-based nanozymes

3.4.1. Modification of MXene-based nanomaterials. Surface modifications, such as functional groups and surface charges,

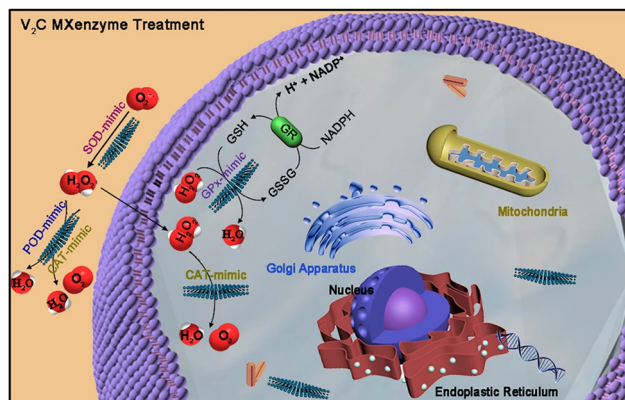


Fig. 5 Schematic illustration of the ROS-scavenging activities of the V_2C nanozyme with multiple enzyme-mimicking properties. Adapted with permission from ref. 85. Copyright (2021) Springer Nature.

can affect the catalytic activities of MXene-based nanozymes. For example, Wu *et al.*³⁷ reported that histidine modification could enhance the POD-like catalytic activity of Ti_3C_2 NSs. Li *et al.*⁷⁵ found that the Ti_3C_2 NSs with a large surface area exhibited intrinsic POD-like activity. Compared to bare Ti_3C_2 NSs, the single-stranded DNA adsorbed on Ti_3C_2 NSs could boost the catalytic properties towards positively charged substrate *o*-phenylenediamine (OPD) oxidation with better affinity and a higher reaction rate.

The catalytic abilities of MXene-based nanozymes can also be tuned by changing the proportion of components in MXenes. MXene nanozymes can achieve enhanced catalytic performances when forming hybrids.⁷³

3.4.2. Environmental regulation. The surrounding temperature can influence the catalytic activities of MXene-based nanozymes.³⁷ Similarly, pH also has a great effect on the catalytic properties.³⁷ The photo-responsive system may also be used to regulate the catalytic efficiencies of MXene-based nanozymes. Due to the high photothermal conversion efficiency of MXenes in the near-infrared (NIR) region, the catalytic properties of MXene nanozyme can increase greatly under NIR irradiation.⁹²

4. Biomedical applications of MXene-based nanozymes

4.1. Biosensing

Nanozymes with POD-like activity have been widely used as biosensors.^{1–3,7–9,24–26} For example, Bhattacharjee *et al.*⁷ integrated the POD-like activity of the synthesized mesoporous iron oxides (MIO) for the detection of global DNA methylation in colorectal cancer cell lines. The target DNA was extracted and denatured to get ssDNA, followed by adsorption onto the surface of a gold electrode; a 5-methylcytosine antibody (5mC)-functionalized MIO (MIO-5mC) was used to recognize the methylcytosine groups; the MIO-5mC conjugates catalyzed TMB in the presence of H_2O_2 to give the colorimetric and electrochemical detection of DNA methylation. The assay has great potential for genome-wide DNA methylation analysis in point-of-care applications.

With good stability, desirable biocompatibility, high conductivity, large surface areas, intriguing enzyme-like activities and the presence of hydrophilic surface groups, MXenes could be functionalized and used to construct useful biosensing platforms. Recently, assays for various bioanalytes like small molecules (for example, glucose, H_2O_2 , *etc.*) and cancer cells have been proposed based on the enzyme-like activities of MXenes.^{73,75–84,92}

4.1.1. Detection of small molecules. Geng *et al.*⁷³ synthesized $\text{Ti}_3\text{C}_2/\text{Pt}$ nanomaterials with enhanced POD-like activity. Using the superior POD-like activity of $\text{Ti}_3\text{C}_2/\text{Pt}$, the colorimetric methods based on the cascade reaction and inhibitory effect were developed for the detection of glucose and glutathione with limits of detection of 1.0 μM and 0.0089 μM , respectively.

Similarly, the $\text{Ti}_3\text{C}_2/\text{CuS}$ nanocomposites⁷⁵ were used for the colorimetric determination of cholesterol with a linear range of 10–100 μM and a limit of detection (LOD) of 1.9 μM . The results showed that the MXene- $\text{Ti}_3\text{C}_2/\text{CuS}$ nanocomposites-based

colorimetric cholesterol biosensor was sensitive, cost-effective, and selective, which had the potential for use in H_2O_2 and cholesterol detection and clinic medical diagnostics.

4.1.2. Detection of proteins. Li *et al.*⁷⁶ developed a simple label-free sensing strategy with Ti_3C_2 NSs for the colorimetric detection of biomolecules. This was based on Ti_3C_2 NSs as a peroxidase-mimic and the ssDNA aptamer as an enzymatic activity enhancement factor along with a recognition substance for the target. In the presence of target biomolecules, the aptamers were desorbed from Ti_3C_2 NSs due to the specific binding of targets to aptamers, thus bringing about a decrease in catalytic activity. Thrombin (TB) as a model was further determined by the constructed biosensor with a linear range of 1.0×10^{-11} to 1.0×10^{-8} M.

In another study, Wu *et al.*³⁷ produced histidine-modified Ti_3C_2 NSs with good POD-like activity. They found that the catalytic process followed Michaelis–Menten behavior, and the NSs showed a higher affinity for substrates as compared to HRP. Based on the POD-like property of Ti_3C_2 NSs, a paper-based colorimetric method integrated with a smartphone to detect glucose was developed. In addition, an immunoassay for the detection of insulin receptor b-subunit (IR-b) was established (Fig. 6).

4.1.3. Detection of cancer cells. Yang *et al.*⁸² constructed a highly sensitive and portable photothermal biosensor for direct capture and detection of circulating tumor cells (CTCs) on a basis of a multifunctional $\text{Ti}_3\text{C}_2@\text{Au}@\text{Pt}$ nanozyme with excellent photothermal properties and high POD-like activity. The $\text{Ti}_3\text{C}_2@\text{Au}@\text{Pt}$ nanocomposites selectively attached to the surface of CTCs through aptamer recognition, which further enhanced the specificity and promoted signal amplification. Thus, the highly sensitive detection of CTCs was successfully achieved in human blood samples. This work showed promising application in the early diagnosis of cancers with the distinct features of high sensitivity, portability, and easy operation of the MXene-based nanozymes.

4.2. Therapeutics

4.2.1. Biocompatibility of MXene-based nanomaterials. For practical applications, it is necessary to analyze MXenes' toxicity and potential environmental risks. In one study, the potential *in vitro* toxicity of the Ti_3C_2 -soybean phospholipid ($\text{Ti}_3\text{C}_2\text{-SP}$) was tested by a CCK-8 assay. After incubating 4T1 cells with $\text{Ti}_3\text{C}_2\text{-SP}$ at various concentrations for 1 and 2 days, the confocal laser scanning microscopy images showed that $\text{Ti}_3\text{C}_2\text{-SP}$ NSs were efficiently uptaken by these cells. There were no obvious side effects on the survival of 4T1 cells, even at the high concentration of 600 $\mu\text{g mL}^{-1}$ of the nanoagent. Further *in vivo* studies showed no detectable pathological toxicity.⁹³

In another study, after hemocompatibility and excretion analysis of the $\text{Ti}_3\text{C}_2\text{-SP}$ structures, no noticeable acute toxicity and high histocompatibility could be detected; these materials are normally excreted out of the body through feces and urine with a total excretory amount of $\sim 10.35\%$.⁹⁴ The $\text{MnO}_x/\text{Ti}_3\text{C}_2$ composites functionalized with SP displayed improved stability along with high biocompatibility and dispersibility.⁹⁵

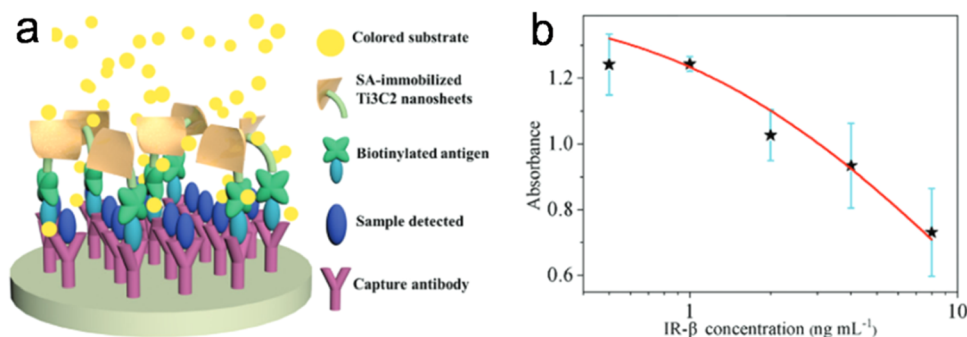


Fig. 6 (a) Schematic illustration of the Ti₃C₂ nanosheet-based immunoassay. (b) Dose–response curves for IR-β detection. Adapted with permission from ref. 37. Copyright (2020) Royal Society of Chemistry.

Possible toxic effects of MXene nanosheets have also been evaluated *in vivo* on zebrafish embryos.⁹⁶ No noticeable teratogenic effects could be detected at 100 μg mL⁻¹. Neurotoxicity evaluations revealed that MXenes had no meaningful toxic effects on neuromuscular activities at 50 μg mL⁻¹. More explorations are necessary to address their long-term biosafety, biodegradation, biocompatibility, and dispersibility.

4.2.2. Therapeutics. MXene-based nanomaterials with enzyme-like properties have been attractive in the fields of immunoassay and therapy.^{92,97–104} For example, Zhu *et al.*⁹² prepared Pt/Ti₃C₂ nanozymes for phototheranostic applications (Fig. 7). The nanomaterials exhibited POD-like activities in the tumor microenvironment to catalyze H₂O₂ for generating •OH to stimulate cell apoptosis. The POD-like activity was highly improved upon NIR-II light irradiation.

In another work, the MXene (Ti₃C₂)/CeO₂-PVP nanomaterials with photo-enhanced dual enzyme-like properties (CAT and

POD) were constructed for synergistic tumor therapy.⁹⁷ The CAT- and POD-like properties of the MXene-based nanozymes alleviated hypoxia and elevated oxidative stress in the tumor microenvironment.

Geng *et al.*⁹⁸ deposited N-doped carbon dots (CDs) onto Nb₂C nanosheets and constructed a mild hyperthermia-enhanced nanocatalytic therapy platform based on Z-scheme heterojunction nanozymes. The CD@Nb₂C nanozymes not only displayed excellent photothermal effects in the second near-infrared (NIR-II) window but also possessed triple enzyme-mimicking activities to obtain amplified ROS levels. The combined therapy effect of the CD@Nb₂C nanozymes through mild NIR-II photothermal-enhanced nanocatalytic therapy could achieve complete tumor eradication. These studies highlighted the 2D multifunctional theranostic nanoplatforms combined with MXene nanocomposites to achieve high nanocatalytic therapeutic outcomes for tumor

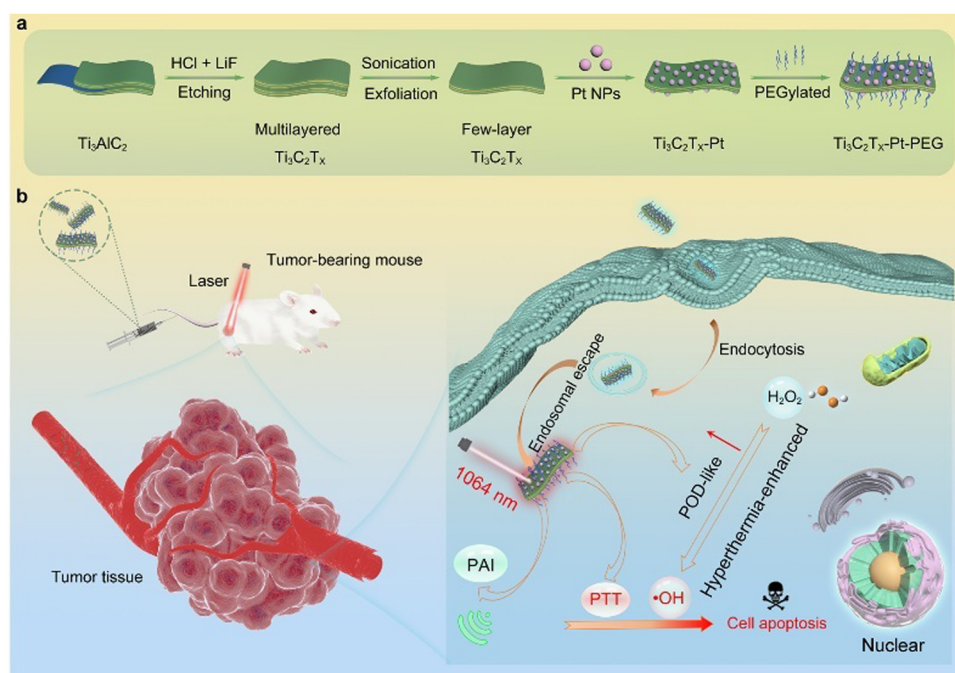


Fig. 7 Schematic diagram showing the design, fabrication, and catalytic-therapeutic properties of Ti₃C₂T_x-Pt-PEG. (a) Illustration of the synthetic procedure for Ti₃C₂T_x-Pt-PEG. (b) The schematic diagram of Ti₃C₂T_x-Pt-PEG with hyperthermia-enhanced nanozyme catalytic activity for cancer therapy. Adapted with permission from ref. 92. Copyright (2022) American Chemical Society.

ablation. At the same time, they also promoted the further development of MXenes in nanomedicine.

4.3. Antibacterial agents

Nanozyme technology has potential applications in infection treatment due to its non-antibiotic dependence. MXene-based nanozymes with POD-like activities have been used for antibacterial applications.^{105–109} For example, Li *et al.*¹⁰⁵ prepared Ti_3C_2 -based nanocomposites by hybridizing Pt single-atom ($\text{Pt}/\text{Ti}_3\text{C}_2$). The single-atom Pt exhibited good POD-like activity to catalyze H_2O_2 and generate hydroxyl radicals, which could kill bacteria and remove biofilms. Moreover, the $\text{Pt}/\text{Ti}_3\text{C}_2$ demonstrated ultrahigh photothermal-conversion efficiency under NIR irradiation at low concentrations. The temperature increase caused by the photothermal effect of the $\text{Pt}/\text{Ti}_3\text{C}_2$ greatly increased the POD-like activity.

Yuan *et al.*¹⁰⁶ designed and constructed a $\text{CeO}_2/\text{Nb}_2\text{C}$ nanozyme with dual functions of POD-like activity and excellent near-infrared (NIR) photothermal properties. Under 808 nm laser irradiation, the $\text{CeO}_2/\text{Nb}_2\text{C}$ produced a photothermal antibacterial effect and also displayed a synergistic enzyme catalytic property, killing bacteria with a sterilization ratio greater than 80%. In a diabetic mouse model, the $\text{CeO}_2/\text{Nb}_2\text{C}$ nanozyme could accelerate the recovery of diabetic wounds when the skin lesions infected with methicillin-resistant *Staphylococcus aureus* were irradiated with an 808 nm laser (Fig. 8).

In another work,¹⁰⁷ vanadium nitride MXenes (*e.g.*, V_2N) were prepared by a modified chemical exfoliation approach. With the valence-switchable state and large specific surface area, the V_2N -based nanomaterials possessed intrinsic OD-like and POD-like activities. In addition, V_2N exhibited desirable photothermal conversion efficiency in the NIR-II window. These

integrated merits enabled the V_2N to generate abundant ROS to effectively eradicate bacteria *in vitro*. These studies have provided a promising strategy based on photothermally enhanced dual enzyme-like catalytic activities for effective anti-infective therapy.

4.4. Antioxidants

The overproduction of reactive oxygen species (ROS) has been involved in the pathogenesis and progression of various human diseases. MXene-based nanozymes have important applications in antioxidants, which can scavenge excessive intracellular ROS to realize powerful cytoprotective effects.^{85–91} For example, the 2D vanadium carbide V_2C nanozyme was constructed to alleviate ROS-mediated inflammatory and neurodegenerative diseases (Fig. 9).⁸⁵ The V_2C nanozyme not only exhibited high biocompatibility but also possessed robust cytoprotection against oxidative damage. Both *in vitro* and *in vivo* experiments verified that the V_2C nanozyme exhibited impressive ROS-scavenging capability to protect cell components against oxidative stress through catalytic reactions.

The V_2C -based nanozymes were also found to have therapeutic potential for treating ischemic stroke.⁸⁶ Zhang *et al.* found that the Mo_2C -based nanozymes could facilitate the elimination of ROS in plasma and cells and the rehabilitation of mice from oxidative stress and mitochondrial dysfunction.⁸⁷

Recently, Yang *et al.*⁹⁰ prepared a Nb_2C nanozyme to fight against hypertension by efficiently eliminating ROS and inhibiting inflammatory factors. They found that the nanozyme displayed multiple enzyme-mimicking activities, including superoxide dismutase, catalase, glutathione peroxidase, and peroxidase. Using a stress-induced hypertension rat model, they demonstrated that Nb_2C nanozymes had cytoprotective effects by resisting oxidative stress, alleviating inflammatory response

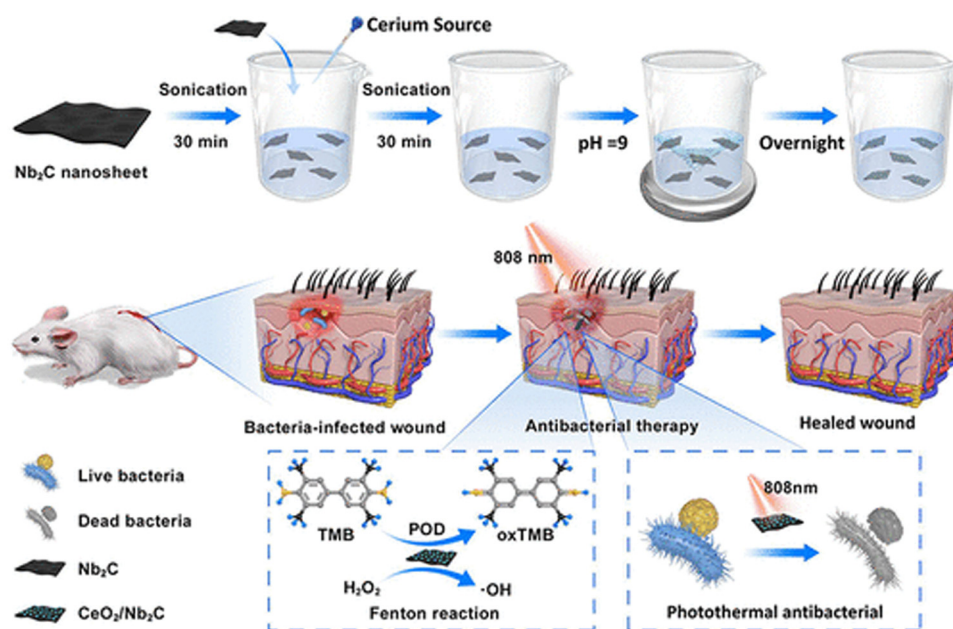


Fig. 8 Schematic of the $\text{CeO}_2/\text{Nb}_2\text{C}$ nanocomposite used to kill pathogens. Adapted with permission from ref. 106. Copyright (2023) American Chemical Society.

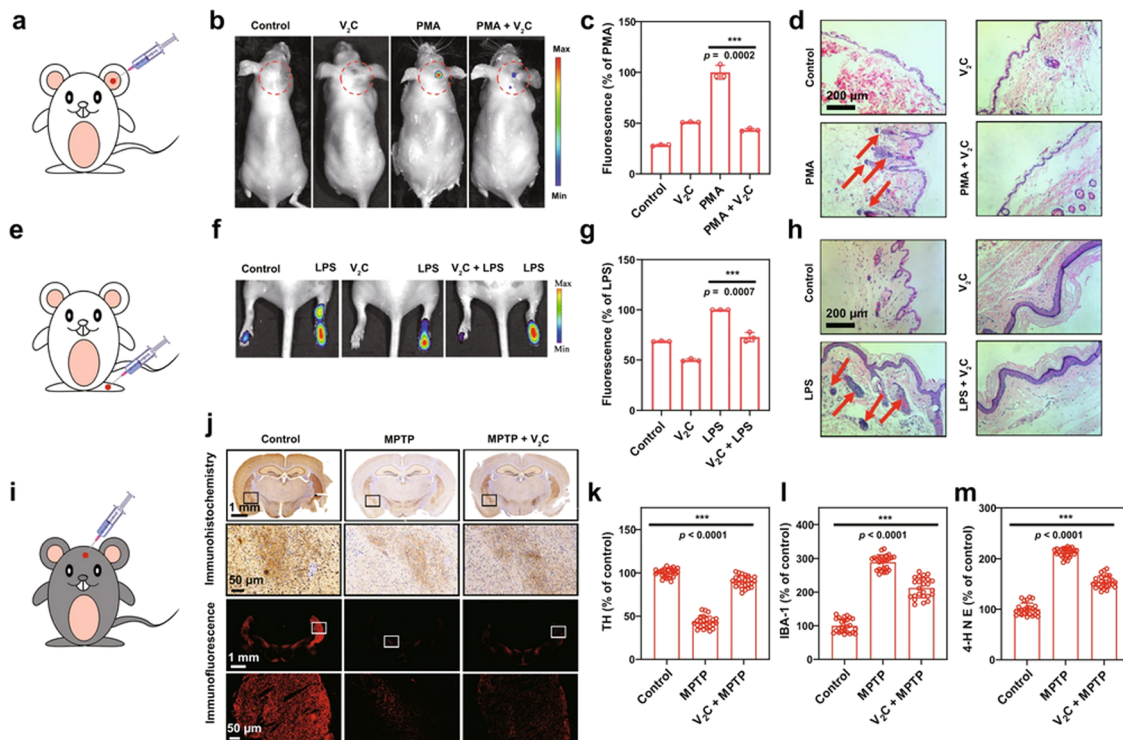


Fig. 9 Inflammation and neurodegeneration therapy based on the V₂C nanozyme. (a) Scheme of ear inflammation model. (b) *In vivo* fluorescence imaging of mice with different treatments to evaluate the effect of V₂C MXenzyme on ROS scavenging in PMA-induced ear inflammation. (c) Corresponding radiant efficiency of the fluorescence images acquired in the live mice after different treatments. (d) H&E-stained images of mice ears after different treatments. (e) Scheme of ankle inflammation model. (f) *In vivo* fluorescence imaging of mice with different treatments to evaluate the effect of V₂C MXenzyme on ROS scavenging in LPS-induced ankle inflammation. (g) Corresponding radiant efficiency of fluorescence images acquired in the live mice after different treatments. (h) H&E-stained images of mice ankles after different treatments. (i) Scheme of PD model treatment. (j) Immunohistochemistry and immunofluorescence images of TH expression in the brains of mice after different treatments (coronal plane). Expression levels of (k) TH, (l) IBA-1, and (m) 4-HNE in each treatment group (coronal plane), quantification represents the ratio of the experimental group to control. Data presented as mean ± SD and asterisks indicate significant differences (***) using one-way analysis of variance (ANOVA). A representative image of three replicates from each group is shown. Adapted with permission from ref. 85. Copyright (2021) Springer Nature.

and reducing blood pressure. These MXene-based theranostic nanozymes showed excellent therapeutic efficacy toward ROS-related brain diseases or other ROS-related inflammatory diseases. Taken together, the MXene-based nanozymes can be used as valuable toolkits for multifarious inflammation and neurodegeneration treatments. These results have extended their biomedical uses from traditional chemical catalysis to catalytic biomedicine.

5. Prospects and challenges

In this mini-review, we have provided a summary of the recent progress of MXene-based nanomaterials with enzyme-like activities for various biomedical applications. The continuous development of MXene-based nanomaterials will offer many opportunities to develop new types of nanozymes with functionalities. At the same time, the integration of the enzyme-like activities of MXene-based nanomaterials with their other functionalities such as photothermal and electric properties will bring limitless applications in biomedical areas.

Despite several achievements made in MXene-based nanozymes, the studies in this field are still in the initial stages and some challenges should be considered in future studies.

(1) It is challenging to control the synthesis of MXene-based nanomaterials with desirable size, uniform thickness, and colloidal stability. It is still desirable to develop an efficient method for preparing MXene-based nanomaterials. The synthesis of MXenes with low hazardous chemicals, low temperature, mild reaction conditions, good dispersibility, and large-scale production still needs to be explored.

(2) The biocompatibility, biodegradation and environmental stability of MXene-based nanomaterials remain largely unknown. Despite several studies on the biocompatibility of Ti₃C₂ MXene nanomaterials, it is desirable to evaluate the toxicity of other types of MXenes. To apply these MXene-based nanomaterials into clinical applications, their biocompatibility, toxicity, and immune reactions are crucial parameters that should be evaluated to fully characterize their safety during clinical translation. The systematic evaluation of the long-term safety of MXene-based nanomaterials is very important for further practical application of these materials in the biomedical field.

(3) Few studies on the in-depth catalytic mechanism of the MXene-based nanozymes are available. It is also hard to design the desired MXene-based nanozymes with optimal structure. More theoretical calculations will be helpful for the structural

design of MXene-based nanozymes by establishing appropriate models for catalysis. Natural enzymes have high binding affinities and substrate specificities. A pocket is available for substrate recognition and catalysis in the active sites of natural enzymes. Therefore, the surface of the MXenes might be coated with functional groups to enhance their substrate specificity and binding affinity.

(4) For the current MXene-based nanozymes, most studies have been performed based on redox reactions, and more MXene-based nanozymes with new catalytic activities beyond oxidative properties are expected. Further investigations are desirable to construct novel MXene-based nanozymes for catalyzing other types of biochemical reactions.

(5) MXene-based hybrid nanomaterials have rich physicochemical properties, such as optical, electrical, thermal, and magnetic properties. They can be applied in the design of multifunctional nanozymes with area-dependent electrocatalytic performances. Bhattacharjee *et al.*⁷ integrated the POD-like activity of the mesoporous iron oxide for the development of a colorimetric and electrochemical platform for DNA methylation detection. They successfully replaced the HRP enzyme with MIO to detect as low as 10% methylation in the complex synthetic samples. By combining the multifunctional properties of MXene-based nanomaterials with enzyme-like activities, the MXene-based nanozymes would provide more efficient and high-performance platforms for practical applications. This direction has not been explored to a great extent, which could be a new and important direction for future studies.

Finally, the current studies on several MXene-based nanozymes with outstanding performances are proof-of-concept. These studies reveal new explorations into the applications of MXene-based nanozymes. There is still a long way to go, and in-depth research is essential for implementing MXene-based nanozymes for practical applications.

Conflicts of interest

There are no conflicts to declare.

Acknowledgements

This work is supported by the Strategic Priority Research Program of the Chinese Academy of Sciences (XDB36000000), the National Key R&D Program of China (2021YFE0112600, 2022YFA1207300), and the National Natural Science Foundation of China (12174032).

References

- L. Z. Gao, J. Zhuang, L. Nie, J. B. Zhang, Y. Zhang, N. Gu, T. H. Wang, J. Feng, D. L. Yang, S. Perrett and X. Y. Yan, *Nat. Nanotechnol.*, 2007, **2**, 577–583.
- H. Wei and E. K. Wang, *Chem. Rev.*, 2013, **42**, 6060–6093.
- Y. Y. Huang, J. S. Ren and X. G. Qu, *Chem. Rev.*, 2019, **119**, 4357–4412.
- D. W. Jiang, D. L. Ni, Z. T. Rosenkrans, P. Huang, X. Y. Yan and W. B. Cai, *Chem. Soc. Rev.*, 2019, **48**, 3683–3704.
- W. W. He, X. C. Wu, J. B. Liu, X. N. Hu, K. Zhang, S. Hou, W. Y. Zhou and S. S. Xie, *Chem. Mater.*, 2010, **22**, 2988–2994.
- X. H. Wang, Q. S. Han, S. F. Cai, T. Wang, R. Yang and C. Wang, *Analyst*, 2017, **142**, 2500–2506.
- R. Bhattacharjee, S. Tanaka, S. Moriam, M. K. Masud, J. Lin, S. M. Alshehri, T. Ahamad, R. R. Salunkhe, N. Nguyen, Y. Yamauchi, M. S. A. Hossain and M. J. A. Shiddiky, *J. Mater. Chem. B*, 2018, **6**, 4783–4791.
- M. K. Masud, J. Kim, M. M. Billah, K. Wood, M. J. A. Shiddiky, N. Nguyen, R. K. Parsapur, Y. Kaneti, A. A. Alshehri, Y. G. Alghamidi, K. A. Alzahrani, M. Adharvanachari, P. Selvam, M. S. A. Hossain and Y. Yamauchi, *J. Mater. Chem. B*, 2019, **7**, 5412–5422.
- M. K. Masud, J. Na, M. Younus, M. Shahriar, A. Hossain, Y. Bando, M. J. A. Shiddiky and Y. Yamauchi, *Chem. Soc. Rev.*, 2019, **48**, 5717–5751.
- W. He, H. Jia, X. Li, Y. Lei, J. Li, H. Zhao, L. Mi, L. Zhang and Z. Zheng, *Nanoscale*, 2012, **4**, 3501–3506.
- Y. Guo, L. Deng, J. Li, S. Guo, E. Wang and S. Dong, *ACS Nano*, 2011, **5**, 1282–1290.
- H. Zhang, *ACS Nano*, 2015, **9**, 9451–9469.
- K. S. Novoselov, A. K. Geim, S. V. Morozov, D. Jiang, Y. Zhang, S. V. Dubonos, I. V. Grigorieva and A. A. Firsov, *Science*, 2004, **306**, 666–669.
- X. R. Gan, H. M. Zhao and X. Quan, *Biosens. Bioelectron.*, 2017, **89**, 56–71.
- X. Q. Huang, S. H. Tang, X. L. Mu, Y. Dai, G. X. Chen, Z. Y. Zhou, F. X. Ruan, Z. L. Yang and N. F. Zheng, *Nat. Nanotechnol.*, 2011, **6**, 28–32.
- S. B. Yang, Y. J. Gong, J. S. Zhang, L. Zhan, L. L. Ma, Z. Y. Fang, R. Vajtai, X. C. Wang and P. M. Ajayan, *Adv. Mater.*, 2013, **25**, 2452–2456.
- Y. J. Ding, Y. P. Chen, X. L. Zhang, L. Chen, Z. H. Dong, H. L. Jiang, H. X. Xu and H. C. Zhou, *J. Am. Chem. Soc.*, 2017, **139**, 9136–9139.
- G. Oudeng, M. Au, J. Shi, C. Wen and M. Yang, *ACS Appl. Mater. Interfaces*, 2018, **10**, 350–360.
- D. T. Ma, J. L. Zhao, J. L. Xie, F. Zhang, R. Wang, L. M. Wu, W. Y. Liang, D. L. Li, Y. Q. Ge, J. Q. Li, Y. P. Zhang and H. Zhang, *Nanoscale Horiz.*, 2020, **5**, 705–713.
- L. Kong, L. Xing, B. Zhou, L. Du and X. Shi, *ACS Appl. Mater. Interfaces*, 2017, **9**, 15995–16005.
- X. L. Lu, X. D. Feng, J. R. Werber, C. H. Chu, I. Zucker, J. H. Kim, C. O. Osuji and M. Elimelech, *Proc. Natl. Acad. Sci. U. S. A.*, 2017, **114**, E9793–E9801.
- Y. J. Song, K. G. Qu, C. Zhao, J. S. Ren and X. G. Qu, *Adv. Mater.*, 2010, **22**, 2206–2210.
- J. P. Wei, X. N. Chen, S. G. Shi, S. G. Mo and N. F. Zheng, *Nanoscale*, 2015, **7**, 19018–19026.
- S. F. Cai, W. Xiao, H. H. Duan, X. X. Liang, C. Wang, R. Yang and Y. D. Li, *Nano Res.*, 2018, **11**, 6304–6315.
- S. F. Cai, Z. Fu, W. Xiao, Y. L. Xiong, C. Wang and R. Yang, *ACS Appl. Mater. Interfaces*, 2020, **12**, 11616–11624.

- 26 H. Y. Sun, X. L. Liu, X. H. Wang, Q. S. Han, C. Qi, Y. M. Li, C. Wang, Y. X. Chen and R. Yang, *Microchim. Acta*, 2020, **187**, 110.
- 27 T. Wang, H. Dong, M. Zhang, T. Wen, J. Meng, J. Liu, Z. Li, Y. Zhang and H. Xu, *Nanoscale*, 2020, **26**, 23084–23091.
- 28 S. F. Cai, J. M. Liu, J. W. Ding, Z. Fu, H. L. Li, Y. L. Xiong, Z. Lian, R. Yang and C. Y. Chen, *Angew. Chem., Int. Ed.*, 2022, **61**, e202204502.
- 29 M. Naguib, O. Mashtalir, J. Carle, V. Presser, J. Lu, L. Hultman, Y. Gogotsi and M. W. Barsoum, *ACS Nano*, 2012, **6**, 1322–1331.
- 30 M. Naguib, M. Kurtoglu, V. Presser, J. Lu, J. Niu, M. Heon, L. Hultman, Y. Gogotsi and M. W. Barsoum, *Adv. Mater.*, 2011, **23**, 4248–4253.
- 31 M. R. Lukatskaya, O. Mashtalir, C. E. Ren, Y. Dall'Agnese, P. Rozier, P. L. Taberna, M. Naguib, P. Simon, M. W. Barsoum and Y. Gogotsi, *Science*, 2013, **341**, 1502–1505.
- 32 J. F. Pang, J. M. Sun, M. Y. Zheng, H. Li, Y. Wang and T. Zhang, *Appl. Catal., B*, 2019, **254**, 510–522.
- 33 Y. Cao, T. T. Wu, K. Zhang, X. Meng, W. Dai, D. Wang, H. Dong and X. Zhang, *ACS Nano*, 2019, **13**, 1499–1510.
- 34 S. Wen, Y. Xiong, S. F. Cai, H. Li, X. Zhang, Q. Sun and R. Yang, *Nanoscale*, 2022, **14**, 16572–16580.
- 35 S. Irvani and R. S. Varma, *Nanomaterials*, 2022, **12**, 1200.
- 36 C. Guan, X. Yue, J. Fan and Q. J. Xiang, *Chin. J. Catal.*, 2022, **43**, 2484.
- 37 X. Wu, T. Chen, Y. Chen and G. Yang, *J. Mater. Chem. B*, 2020, **8**, 2650–2659.
- 38 C. L. Tan, X. H. Cao, X. J. Wu, Q. Y. He, J. Yang, X. Zhang, J. Z. Chen, W. Zhao, S. K. Han, G. H. Nam, M. Sindoro and H. Zhang, *Chem. Rev.*, 2017, **117**, 6225–6331.
- 39 Y. Chen, C. L. Tan, H. Zhang and L. Z. Wang, *Chem. Soc. Rev.*, 2015, **44**, 2681–2701.
- 40 C. Xu, L. Wang, Z. Liu, L. Chen, J. Guo, N. Kang, X. Ma, H. Cheng and W. Ren, *Nat. Mater.*, 2015, **14**, 1135–1141.
- 41 W. Tang, Z. Dong, R. Zhang, X. Yi, K. Yang, M. Jin, C. Yuan, Z. Xiao, Z. Liu and L. Cheng, *ACS Nano*, 2019, **13**, 284–294.
- 42 J. Wang, X. Wei, X. Wang, W. Song, W. Zhong, M. Wang, J. Ju and Y. Tang, *Inorg. Chem.*, 2021, **60**, 5890–5897.
- 43 T. Wojciechowski, A. Rozmysłowska-Wojciechowska, G. Matyszczyk, M. Wrzcionek, A. Olszyna, A. Peter, A. Mihaly-Cozmuta, C. Nicula, L. Mihaly-Cozmuta, S. Podsiadlo, D. Basiak, W. Ziemkowska and A. Jastrzębska, *Inorg. Chem.*, 2019, **58**, 7602–7614.
- 44 M. Alhabeb, K. Maleski, B. Anasori, P. Lelyukh, L. Clark, S. Sin and Y. Gogotsi, *Chem. Mater.*, 2017, **29**(18), 7633–7644.
- 45 L. Verger, C. Xu, V. Natu, H. Cheng, W. Ren and M. W. Barsoum, *Curr. Opin. Solid State Mater. Sci.*, 2019, **23**, 149–163.
- 46 M. Naguib, O. Mashtalir, J. Carle, V. Presser, J. Lu, L. Hultman, Y. Gogotsi and M. W. Barsoum, *ACS Nano*, 2012, **6**(2), 1322–1331.
- 47 M. H. Tran, T. Schäfer, A. Shahraei, M. Dürrschnabel, L. Molina-Luna, U. I. Kramm and C. S. Birkel, *ACS Appl. Energy Mater.*, 2018, **1**, 3908–3914.
- 48 A. VahidMohammadi, A. Hadjikhani, S. Shahbazmohamadi and M. Beidaghi, *ACS Nano*, 2017, **11**, 11135–11144.
- 49 S. S. Zhao, X. Meng, K. Zhu, F. Du, G. Chen, Y. J. Wei, Y. Gogotsi and Y. Gao, *Energy Storage Mater.*, 2017, **8**, 42–48.
- 50 J. Zhou, X. Zha, X. Zhou, F. Chen, G. Gao, S. Wang, C. Shen, T. Chen, C. Zhi, P. Eklund, S. Du, J. Xue, W. Shi, Z. Chai and Q. Huang, *ACS Nano*, 2017, **11**, 3841–3850.
- 51 B. Soundiraraju and B. K. George, *ACS Nano*, 2017, **11**, 8892–8900.
- 52 M. Ghidui, M. R. Lukatskaya, M. Q. Zhao, Y. Gogotsi and M. W. Barsoum, *Nature*, 2014, **516**, 78–81.
- 53 F. Liu, A. Zhou, J. Chen, J. Jia, W. Zhou, L. Wang and Q. Hu, *Appl. Surf. Sci.*, 2017, **416**, 781–789.
- 54 F. Liu, J. Zhou, S. Wang, B. Wang, C. Shen, L. Wang, Q. Hu, Q. Huang and A. Zhou, *J. Electrochem. Soc.*, 2017, **164**, A709–A713.
- 55 J. Halim, M. R. Lukatskaya, K. M. Cook, J. Lu, C. R. Smith, L. Näslund, S. J. May, L. Hultman, Y. Gogotsi, P. Eklund and M. W. Barsoum, *Chem. Mater.*, 2014, **26**, 2374–2381.
- 56 A. Lipatov, M. Alhabeb, M. R. Lukatskaya, A. Boson, Y. Gogotsi and A. Sinitskii, *Adv. Electron. Mater.*, 2016, **2**, 1600255.
- 57 M. Li, J. Lu, K. Luo, Y. Li, K. Chang, K. Chen, J. Zhou, J. Rosen, L. Hultman, P. Eklund, P. Persson, S. Du, Z. Chai, Z. Huang and Q. Huang, *J. Am. Chem. Soc.*, 2019, **141**, 4730–4737.
- 58 Y. Li, H. Shao, Z. Lin, J. Lu, L. Liu, B. Duployer, P. O. Å. Persson, P. Eklund, L. Hultman, M. Li, K. Chen, X. Zha, S. Du, P. Rozier, Z. Chai, E. Raymundo-Piñero, P. Taberna, P. Simon and Q. Huang, *Nat. Mater.*, 2020, **19**, 894–899.
- 59 T. Li, L. Yao, Q. Liu, J. Gu, R. Luo, J. Li, X. Yan, W. Wang, P. Liu, B. Chen, W. Zhang, W. Abbas, R. Naz and D. Zhang, *Angew. Chem. Int. Ed.*, 2018, **57**, 6115–6119.
- 60 J. Xuan, Z. Wang, Y. Chen, D. Liang, L. Cheng, X. Yang, Z. Liu, R. Ma, T. Sasaki and F. Geng, *Angew. Chem. Int. Ed.*, 2016, **55**, 14569–14574.
- 61 J. N. Xuan, Z. Q. Wang, Y. Y. Chen, D. J. Liang, L. Cheng, X. J. Yang, Z. Liu, R. Z. Ma, T. Sasaki and F. X. Geng, *Angew. Chem. Int. Ed.*, 2016, **55**, 14569–14574.
- 62 H. Lin, X. Wang, L. Yu, Y. Chen and J. Shi, *Nano Lett.*, 2017, **17**, 384–391.
- 63 X. Wu, L. Hao, J. Zhang, X. Zhang and J. Wang, *J. Membr. Sci.*, 2016, **515**, 175–188.
- 64 J. Yan, C. E. Ren, K. Maleski, C. B. Hatter, B. Anasori, P. Urbankowski, A. Sarycheva and Y. Gogotsi, *Adv. Funct. Mater.*, 2017, **27**, 1701264.
- 65 B. Ahmed, D. H. Anjum, Y. Gogotsi and H. N. Alshareef, *Nano Energy*, 2017, **34**, 249–256.
- 66 Y. Wu, P. Nie, J. Jiang, B. Ding, H. Dou and X. Zhang, *ChemElectroChem*, 2017, **4**, 1560–1565.
- 67 D. Chen, S. Shao, W. Zhang, J. Zhao and M. Lian, *Chim. Acta*, 2022, **1197**, 339520.
- 68 M. Iqbal, J. Fatheema, Q. Noor, M. Rani, M. Mumtaz, R. Zheng, S. Ayaz Khan and S. Rizwan, *Mater. Today Chem.*, 2020, **16**, 100271.

- 69 S. Yao, B. Anasori and A. Strachan, *J. Appl. Phys.*, 2022, **132**, 204301.
- 70 R. B. Rakhi, P. Nayak, C. Xia and H. N. Alshareef, *Sci. Rep.*, 2016, **6**, 36422.
- 71 H. Geng, Z. Li, Q. Liu, Q. Yang, H. Jia, Q. Chen, A. Zhou and W. He, *Dalton Trans.*, 2022, **51**, 11693–11702.
- 72 W. Tang, Z. Dong, R. Zhang, X. Yi, K. Yang, M. Jin, C. Yuan, Z. Liu and L. Cheng, *ACS Nano*, 2019, **13**, 284–294.
- 73 J. Wang, X. Wei, X. Wang, W. Song, W. Zhong, M. Wang, J. Ju and Y. Tang, *Inorg. Chem.*, 2021, **60**, 5890–5897.
- 74 T. Wojciechowski, A. Rozmysłowska-Wojciechowska, G. Matyszczyk, M. Wrzeciećek, A. Olszyna, A. Peter, A. Mihaly-Cozmuta, C. Nicula, L. Mihaly-Cozmuta, S. Podsiadło, D. Basiak, W. Ziemkowska and A. Jastrzębska, *Inorg. Chem.*, 2019, **58**, 7602–7614.
- 75 Y. Li, Z. Kang, L. Kong, H. Shi, Y. Zhang, M. Cui and D. Yang, *Mater. Sci. Eng., C*, 2019, **104**, 110000.
- 76 M. Li, X. Peng, Y. Han, L. Fan, Z. Liu and Y. Guo, *Microchem. J.*, 2021, **166**, 106238.
- 77 Z. Jin, G. Xu, Y. Niu, X. Ding, Y. Han, W. Kong, Y. Fang, H. Niu and Y. Xu, *J. Mater. Chem. B*, 2020, **8**, 3513–3518.
- 78 J. Guo, G. Wang, J. Zou and Z. Lei, *Anal. Bioanal. Chem.*, 2023, **415**, 3559–3569.
- 79 Z. Lei, J. Guo, J. Zou and Z. Wang, *Microchim. Acta*, **189**, 369.
- 80 L. Yu, J. Chang, X. Zhuang, H. Li, T. Hou and F. T. Li, *Anal. Chem.*, 2022, **94**, 3669–3676.
- 81 J. Wang, W. Xu, L. Zhou, T. Zhang, N. Yang, M. Wang, X. Luo, L. Jin, H. Zhu and W. Ge, *Microchim. Acta*, 2022, **189**, 452.
- 82 L. Yang, H. Guo, T. Hou, J. Zhang and F. Li, *Biosens. Bioelectron.*, 2023, **234**, 115346.
- 83 X. Xi, J. Wang, Y. Wang, H. Xiong, M. Chen, Z. Wu, X. Zhang, S. Wang and W. Wen, *Carbon*, 2022, **197**, 476–484.
- 84 D. Chen, S. Shao, W. Zhang, J. Zhao and M. Lian, *Anal. Chim. Acta*, 2022, **1197**, 339520.
- 85 W. Feng, X. G. Han, H. Hu, M. Q. Chang, L. Ding, H. J. Xiang, Y. Chen and Y. H. Li, *Nat. Commun.*, 2021, **12**, 1–16.
- 86 H. Hu, H. Huang, L. Xia, X. Qian, W. Feng, Y. Chen and Y. Li, *Chem. Eng. J.*, 2022, **440**, 135810.
- 87 D. Zhang, L. Jiang, L. Li, X. Li, W. Zheng, L. Gui, Y. Yang, Y. Liu, L. Yang, J. Wang, Y. Xiong, L. Ji, Y. Deng, X. Liu, Q. He, X. Hu, X. Liu, R. Fan, Y. Lu, J. Liu, J. Cheng, H. Yang, T. Li and M. Gong, *Biomaterials*, 2022, **287**, 121678.
- 88 C. Du, W. Feng, X. Dai, J. Wang, D. Geng, X. Li, Y. Chen and J. Zhang, *Small*, 2022, **18**, e2203031.
- 89 H. Geng, Y. Ren, G. Qin, T. Wen, Q. Liu, H. Xu and W. He, *RSC Adv.*, 2022, **12**, 11128–11138.
- 90 H. Yang, L. Xia, X. Ye, J. Xu, T. Liu, L. Wang, S. Zhang, W. Feng, D. Du and Y. Chen, *Angew. Chem., Int. Ed.*, 2023, **62**, e202303539.
- 91 X. Y. Ren, M. F. Huo, M. M. Wang, H. Lin, X. Zhang, J. Yin, Y. Chen and H. Chen, *ACS Nano*, 2019, **13**, 6438–6454.
- 92 Y. Zhu, Z. Wang, R. Zhao, Y. Zhou, L. Feng, S. Gai and P. Yang, *ACS Nano*, 2022, **16**, 3105–3118.
- 93 X. Lin, L. Wang, L. Yu, Y. Chen and J. Shi, *Nano Lett.*, 2017, **17**, 384–391.
- 94 X. Han, J. Huang, H. Lin, Z. Wang, P. Li and Y. Chen, *Adv. Healthcare Mater.*, 2018, **7**, 1701394.
- 95 C. Dai, H. Lin, G. Xu, Z. Liu, R. Wu and Y. Chen, *Chem. Mater.*, 2017, **29**, 8637–8652.
- 96 G. K. Nasrallah, M. Al-Asmakh, K. Rasool and K. A. Mahmoud, *Environ. Sci.: Nano*, 2018, **5**, 1002–1011.
- 97 M. Tang, Y. Shi, L. Lu, J. Li, Z. Zhang, J. Ni, W. Wang, Y. Zhang, T. Sun and Z. Wu, *Chem. Eng. J.*, 2022, **449**, 137847.
- 98 B. Geng, L. Yan, Y. Zhu, W. Shi, H. Wang, J. Mao, L. Ren, J. Zhang, Y. Tian, F. Gao, X. Zhang, J. Chen and J. Zhu, *Adv. Healthcare Mater.*, 2022, **12**, 2202154.
- 99 Z. Hao, Y. Li, X. Liu, T. Jiang, Y. He, X. Zhang, C. Cong, D. Wang, Z. Liu and D. Gao, *Chem. Eng. J.*, 2021, **425**, 130639.
- 100 J. Li, X. Cai, Y. Zhang, K. Li, L. Guan, Y. Li, T. Wang and T. Sun, *ChemistrySelect*, 2022, **7**, e202201127.
- 101 X. Zhang, L. Cheng, Y. Lu, J. Tang, Q. Lv, X. Chen, Y. Chen and J. Liu, *Nano-Micro Lett.*, 2022, **14**, 22.
- 102 X. Chang, Q. Wu, Y. Wu, X. Xi, J. Cao, H. Chu, Q. Liu, Y. Li, W. Wu, X. Fang and F. Chen, *Nano Lett.*, 2022, **22**, 8321–8330.
- 103 Y. Zhu, Z. Wang, R. Zhao, Y. Zhou, L. Feng, S. Gai and P. Yang, *ACS Nano*, 2022, **16**, 3105–3118.
- 104 Y. Liang, C. Liao, X. Guo, G. Li, X. Yang, J. Yu, J. Zhong, Y. Xie, L. Zheng and J. Zhao, *Small*, 2023, **32**, 2205511.
- 105 Z. Li, D. Xu, Z. Deng, J. Yin, Y. Qian, J. Hou, X. Ding, J. Shen and X. He, *Chem. Eng. J.*, 2023, **452**, 139587.
- 106 H. Yuan, X. Hong, H. Ma, C. Fu, Y. Guan, W. Huang, J. Ma, P. Xia, M. Cao, L. Zheng, X. Xu, C. Xu, D. Liu, Z. Li, Q. Geng and J. Wang, *ACS Mater. Lett.*, 2023, **5**, 762–774.
- 107 X. Sun, X. He, Y. Zhu, E. Obeng, B. Zeng, H. Deng, J. Shen and R. Hu, *Chem. Eng. J.*, 2023, **451**, 138985.
- 108 G. Sun, X. Jiang, C. Liu, S. Song, J. Zhang and J. Shen, *Nano Res.*, 2023, **16**, 2840–2850.
- 109 J. Shi, R. Shu, X. Shi, Y. Li, J. Li, Y. Deng and W. Yang, *RSC Adv.*, 2022, **12**, 11090–11099.